



## Reducing Roof Solar Heat Gain by Using Double-Skin Ventilated Roofs

Mohannad R. Ghanim <sup>a\*</sup>, Sabah T. Ahmed <sup>b</sup>

<sup>a</sup> University of Technology, Mechanical Engineering Department, Baghdad, Iraq.  
[mohannad.rushdi@gmail.com](mailto:mohannad.rushdi@gmail.com)

<sup>b</sup> University of Technology, Mechanical Engineering Department, Baghdad, Iraq

\*Corresponding author.

Submitted: 15/07/2019

Accepted: 07/09/2019

Published: 25/03/2020

### KEYWORDS

Double skin roof, free convection, naturally ventilated, passive cooling, ventilated roof.

### ABSTRACT

Double skin ventilated roof is one of the important passive cooling techniques to reduce solar heat gain through roofs. In this research, an experimental study was performed to investigate the thermal behaviour of a double skin roof model. The model was made of two parallel galvanized steel plates. Galvanized steel has been used in the roof construction of industrial buildings and storehouses in Iraq. The effect of inclination angle ( $\theta$ ) from the horizontal and the spacing ( $S$ ) between the plates was investigated at different radiation intensities. It is found that using a double skin roof arrangement with a sufficient air gap ( $S$ ) can reduce the heat gain significantly. The higher the inclination angle ( $\theta$ ) the higher the ventilation rate, the lower the heat gain through the roof. In this study, increasing the air gap from 2 cm to 4 cm reduced the heat gain significantly but when the gap was further increased to 6 cm, the reduction in the heat flux was insignificant. A dimensionless correlation was also reduced between Nusselt number ( $Nu_S$ ) and the single parameter  $Ra_S^* \sin \theta (S/L)$  where  $L$  is the channel length. This correlation can be handily utilized for designing of engineering applications dealing with high temperature difference natural convection heat transfer.

**How to cite this article:** M. R. Ghanim and S. T. Ahmed, "Reducing roof solar heat gain by using double-skin ventilated roofs," *Engineering and Technology Journal*, Vol. 38, Part A, No. 03, pp. 402-411, 2020.

DOI: <https://doi.org/10.30684/etj.v38i3A.462>

### 1. Introduction

Roofs of buildings during summer are highly susceptible to the solar radiation and therefore receive large amounts of heat, which will pass through the roof to the indoor and accounts for a large portion of the total cooling load of the building. Clearly, this causes a serious challenge of overheating, hence making the cooling of the building too expensive. Usually, the proposed solution is the over insulation of buildings that form huge thermal storage and subsequently affects the indoor thermal comfort. Therefore, it is cost effective to develop alternative construction techniques that ensure both thermal comfort for

inhabitants and low energy use. One of the important passive cooling techniques is double skin ventilated roof system. It consists of two solid parallel layers, one on top and the other at the bottom separated by an air gap. The upper layer shields the lower one from direct solar radiation, and the air gap works as an insulation layer. The accumulated heat transferred from the upper layer can be removed naturally by tilting the roof in order to induce an upward flow of air due to the buoyancy effect as shown in Figure 1. A literature review shows that many experimental studies have been performed regarding this technique. For example, Hirunlabh et al. [1] discussed the performance of a roof model which consisted of modern materials, a CPAC Monier (concrete tiles for roofing) as the upper skin and a gypsum board as the lower skin. They concluded that this roof could be used to induce air circulation within the roof, which will significantly reduce the heat accumulation between the two skins. The following year, Khadari et al. [2] developed a test rig for estimating the internal convective heat transfer coefficient. They varied the upper plate temperature between 40°C and 75°C and found that the mean convection heat transfer coefficient varies between 6.76 and 10.26 W/m<sup>2</sup>.K accordingly. In 2004, Bunnag et al. [3] made a similar study with a 1 m wide and 1.5 m length channel. They studied two air gaps and five tilt angles at three heat fluxes and they finally reduced correlations between Reynolds and Nusselt numbers as a function of Rayleigh number, channel aspect ratio, and tilt angle. Paungsombut et al. [4] performed experiments with another double skin roof and concluded that placing a radiant barrier on the lower skin could reduce the heat gain by about 50%. The next year, C.-m. Lai et al. [5] approved the same and concluded that the optimal gap between the skins when the maximum heat is ventilated is close to the sum of the thermal boundary layer thickness of the plates. At the same time, Susanti et al. [6] have worked on the effect of airflow resistance in practical applications by varying the outlet and inlet opening size and found that higher resistances cause low velocity and temperature rise. While Salman and Hamad [7] have studied the laminar natural convection heat transfer between two parallel plates on a small experimental apparatus of 360 mm length and 150 mm width and stated the effect of varying the spacing between the plates at different heat fluxes. In 2009, Lee et al. [8] evaluated the influence of panel profiles and found that using ribbed panels as the upper skin increases the temperature of the lower surface. In 2014, S. Tong and H. Li [9] showed that the most influential double skin roof parameters are the reflectance of the upper outer surface and the emittance of the cavity surfaces, followed by the thermal resistance of the lower skin, thermal resistance upper skin, roof inclination and air gap thickness. In 2017, Bokor et al. [10] presented a developed passive cooling roof type, namely Transpired Solar Collector TSC. They used a perforated metal plate as the upper skin, which absorbs the solar radiation and heats up the ventilation air. They proved that the heat gain of the lower skin is significantly lower than that received on the exposed roof.

The aim of this research is to investigate experimentally the thermal behaviour of a double skin roof model that is made of different material, two parallel inclined galvanized steel sheets. Galvanized steel is widely used in Iraq in the roof construction of industrial buildings and storehouses.

## 2. The Experimental Setup

The experimental rig is well designed and constructed for the purpose of the study. As illustrated in Figure 2, it consists mainly of four major parts, the stand, the roof model, the sun simulator, and the control panel. The upper part of the stand is movable to adjust the inclination angle of the roof. The roof model includes two identical parallel galvanized steel sheets of 1.5 m long, 0.6 m wide and 1 mm thickness, as shown in Figure 3 and 4, and two side wood plates of 1cm thickness followed by a layer of 5 cm extruded polystyrene (XPS) insulation board to neglect the flow of heat in the third direction. The air gap thickness can be adjusted between (0.02, 0.04, and 0.06 m) by mounting the lower plate on different support pins. The experiments were performed indoor to exclude the effect of wind and to avoid testing in variant sunlight conditions and standardize the testing environment. Therefore, a sun simulator had to be used to simulate solar radiation. It was consisted of a set of eight 500W/2A/220V tungsten halogen lighting bulbs. Tungsten halogen lamps have been used in the construction of commercial solar simulators [11]. They have also been used before by many researchers for the same purpose [5,12,13]. The electromagnetic wavelengths of these bulbs fall between 0.38 and 3 μm [12], which are almost the same wavelengths of the solar radiation received on the ground. They were distributed in such a way that ensures almost uniform heat flux over the upper plate. A solid-state relay was connected to the lightings with a variable resistor to make the study at different radiation intensities. The electrical power was fed to the system from a stabilizer to provide a stable voltage and secure power supply and to avoid the variation in the radiation intensity.

All the electrical accessories were fixed on a wood board and attached to the rig body, as shown in Figure 2a.

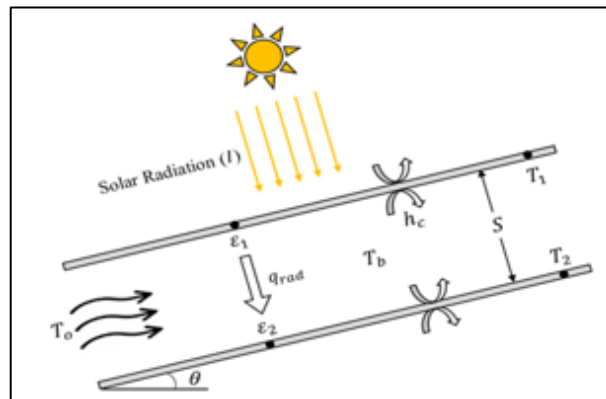


Figure 1: Heat transfer mechanism across a double skin ventilated roof



Figure 2: The experimental rig. (a) Photographic image. (b) Isometric view

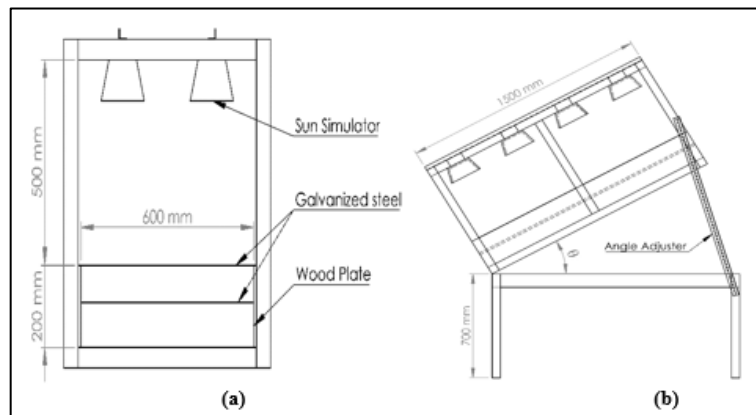


Figure 3: Schematics of the experimental rig. (a) Side view. (b) Front view

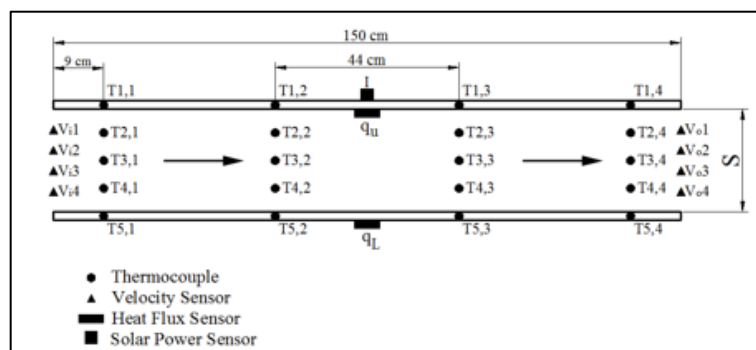


Figure 4: Schematic of sensors distribution in the roof model

### I. Measurements

All the measurements made are in terms of temperature, velocity, irradiance and heat flux. Type-K calibrated thermocouples were used to measure the temperature in twenty different places, four on each plate to estimate the average temperature of them and twelve thermocouples were distributed in the air gap along three imaginary planes (four thermocouples in each plane) to study the temperature distribution between the two plates and also estimate the mean bulk air temperature, as shown in Figure 4. All thermocouples were connected to a digital thermometer type (TM-903A) from LUTRON ELECTRONIC through a COMARK selector switch (20 channel). The air velocity was measured in eight different places, four at the inlet and four at the outlet by an HT-9829 Hot Wire Anemometer. The radiation intensity fallen on the roof model was measured with a solar power meter model SPM-1116SD. Regarding the heat flux transferred through the upper and lower plates, it was measured using two items of PHFS-01 heat flux sensor and its FluxDAQ reader from FluxTeq. All readings were taken after the system reached a steady state condition. The emissivity of the galvanized steel sheet was measured at the Iraqi ministry of science and technology by a TIR100-2 Emissometer and it's found to be 0.025.

### II. Theory

Two-dimensional analysis of the data measured was conducted to estimate the free convection heat transfer within the rectangular channel by forming a correlation between Nusselt number ( $Nu_S$ ) as a function of the modified Rayleigh number ( $Ra_S^*$ ), inclination angle ( $\theta$ ), and aspect ratio defined as air gap thickness to channel length ( $S/L$ ) as follows [14]:

$$Nu_S = \frac{h_c S}{k} = A \left[ Ra_S \sin \theta \left( \frac{S}{L} \right) \right]^B \quad (1)$$

Where  $Ra_S^*$  is defined as [14]:

$$Ra_S^* = \frac{g \beta q_u S^4}{k \nu \alpha} \quad (2)$$

Where  $g$  is the acceleration of gravity,  $\beta$  is the thermal expansion coefficient of air ( $1/T_b$  (K)),  $q_u$  is the uniform heat flux from the upper plate,  $k$  is the thermal conductivity of air,  $\nu$  is the kinematic viscosity of air,  $\alpha$  is the thermal diffusivity of air. All air properties were calculated as a function of air bulk temperature ( $T_b$ ). Regarding the convection heat transfer coefficient  $h_c$ , it can be defined as [14]:

$$h_c = \frac{1}{T_1 - T_b} \left[ q_u - \frac{\sigma(T_1^4 - T_2^4)}{\frac{1}{\epsilon_1} + \frac{1}{\epsilon_2} - 1} \right] \quad (3)$$

Where  $T_1$  and  $T_2$  are the average temperature of the upper and lower plate, respectively,  $T_b$  is the air bulk temperature,  $\epsilon_1$  and  $\epsilon_2$  are the emissivity of the upper and lower plate surfaces. The above temperatures are calculated by the appropriate numerical integration methods [15], (see Appendix A). For comparison purposes, the overall heat transfer coefficient was evaluated to estimate how much heat the roof model was transmitting by taking the average value for different radiation intensities:

$$U = \frac{q_L}{T_1 - T_2} \quad (4)$$

## 3. Results and Discussions

### I. The effect of placing another roof skin

A single plate roof arrangement was first exposed to the direct radiation and the transferred heat flux was measured. The results were compared with that obtained after placing the lower plate at different elevations as shown in Figure 5. It turned out that placing another skin significantly reduced the heat transferred through the roof as the upper plate shields the lower plate from direct radiation and the air gap works as an insulation layer. Since the roof is tilted at a specific angle, the heat transferred from the upper plate to the air gap is continuously dissipated due to the buoyancy effect.

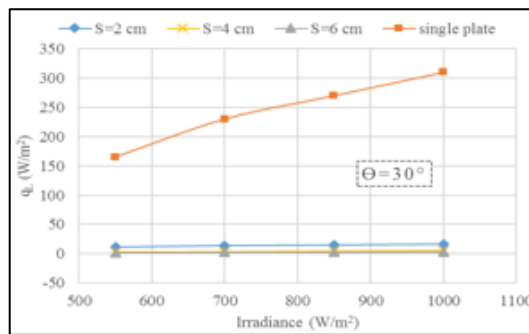


Figure 5: Comparison of the transferred heat flux between different roof model arrangements

## II. The temperature variation

The common observed temperature profiles along the length of the channel are illustrated in Figure 6. The temperature of the upper heated plate and the lower plate increased quasi-linearly from the inlet to the outlet. The air temperature of the layers within the channel similarly increased following the constant heat flux coming from the heated plate. It could be noticed that the air temperature increased quickly at the entrance due to the significant temperature difference between the air and the heated plate. This behaviour has been observed before by Bunnag et al. [3] and Puangsombut et al. [4].

## III. The velocity variation

Assuming no slip conditions at the wall, the measured velocities showed that the velocity profiles are almost uniform at the cavity inlet while they vary from a maximum near the upper plate and decrease gradually toward the lower plate at the cavity outlet as shown in Figure 7. This is due to the variation of air density between the warmer air and cooler air within the cavity. This observation is identical to that observed by Tong and Li [9]. Increasing the inclination angle from  $10^\circ$  to  $30^\circ$  increased the average velocity while varying the air gap between the plates slightly affected the average velocity, which depends on the amount of heated air in the air gap and the wall shear stress.

## IV. The effect of inclination angle

Two angles ( $10^\circ$  and  $30^\circ$ ) were examined as they are the less and the most tilting angles those have been used in pitch roofs construction. Increasing the inclination angle from  $10^\circ$  to  $30^\circ$  increased the ventilation rates of the air cavity as air particles find their way up faster, thus more heat is dissipated, and hence less heat flux was transferred through the ceiling, as shown in Figure 8. Regarding the average convection heat transfer coefficient at the upper internal surface, it increased when the inclination angle increased due to the increased flow velocity near the wall. Subsequently, Nusselt number ( $Nu_c$ ) was also higher for higher inclinations indicating that heat is transferred mainly by convection as compared with conduction. Similarly, the modified Rayleigh number increased when the inclination angle increased from  $10^\circ$  to  $30^\circ$  due to the increased flow velocity and hence more instability is experienced. As shown in Figure 9, the increase in the convection heat transfer coefficient when the inclination was increased from  $10^\circ$  to  $30^\circ$  is higher when the air gap is 6 cm until the angle has no effect on the average convection heat transfer coefficient at 2 cm air gap, that is due to the increased bulk temperature of air. The effect of inclination angle on the overall heat transfer coefficient of the roof model is illustrated in Figure 10.

## V. The effect of air gap thickness

Three thicknesses of the air gap, namely (2, 4, and 6 cm) were investigated. Increasing the air gap from 2 cm to 6 cm reduced the heat flux transferred through the lower plate as shown in Figure 8. The reduction of heat flux was insignificant when the gap increased from 4 cm to 6 cm because the lower plate was sufficiently far from the hot temperature gradient above it. As for the convection heat transfer coefficient, it increased when the air gap decreased from 6 cm to 4 cm due to the increased average flow velocity within the space, but it decreased when the air gap further decreased to 2 cm as the bulk temperature of air rose up as shown in Figure 9. The modified Rayleigh number was also directly proportional to the air gap because the flow path is guided within the narrow channel and hence the instability was decreased as shown in Figure 11. The effect of the air gap thickness on the overall heat transfer coefficient of the roof model is illustrated in Figure 10.

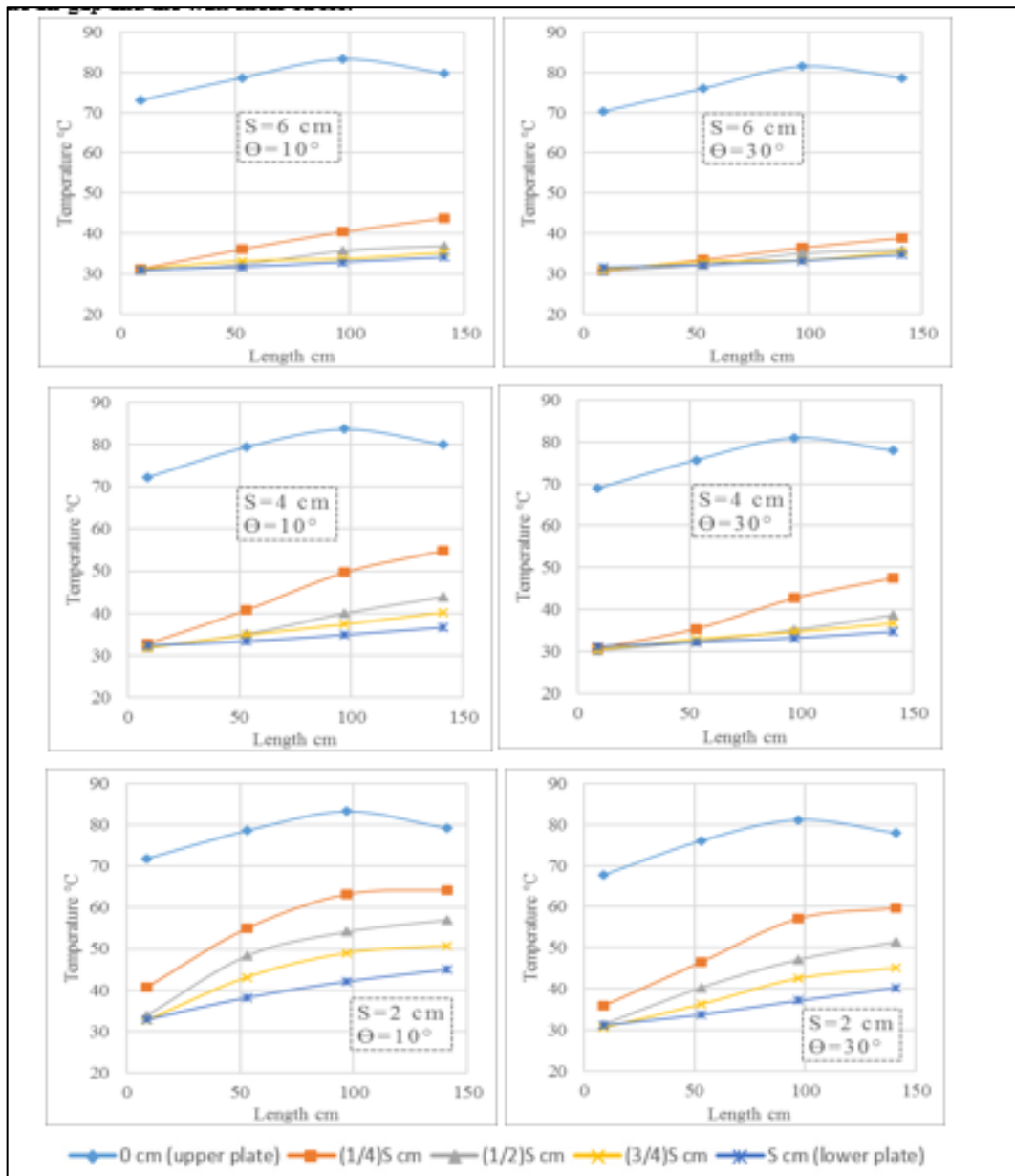


Figure 6: Temperature variation along the length of the channel at  $1000 \text{ W/m}^2$  radiation intensity

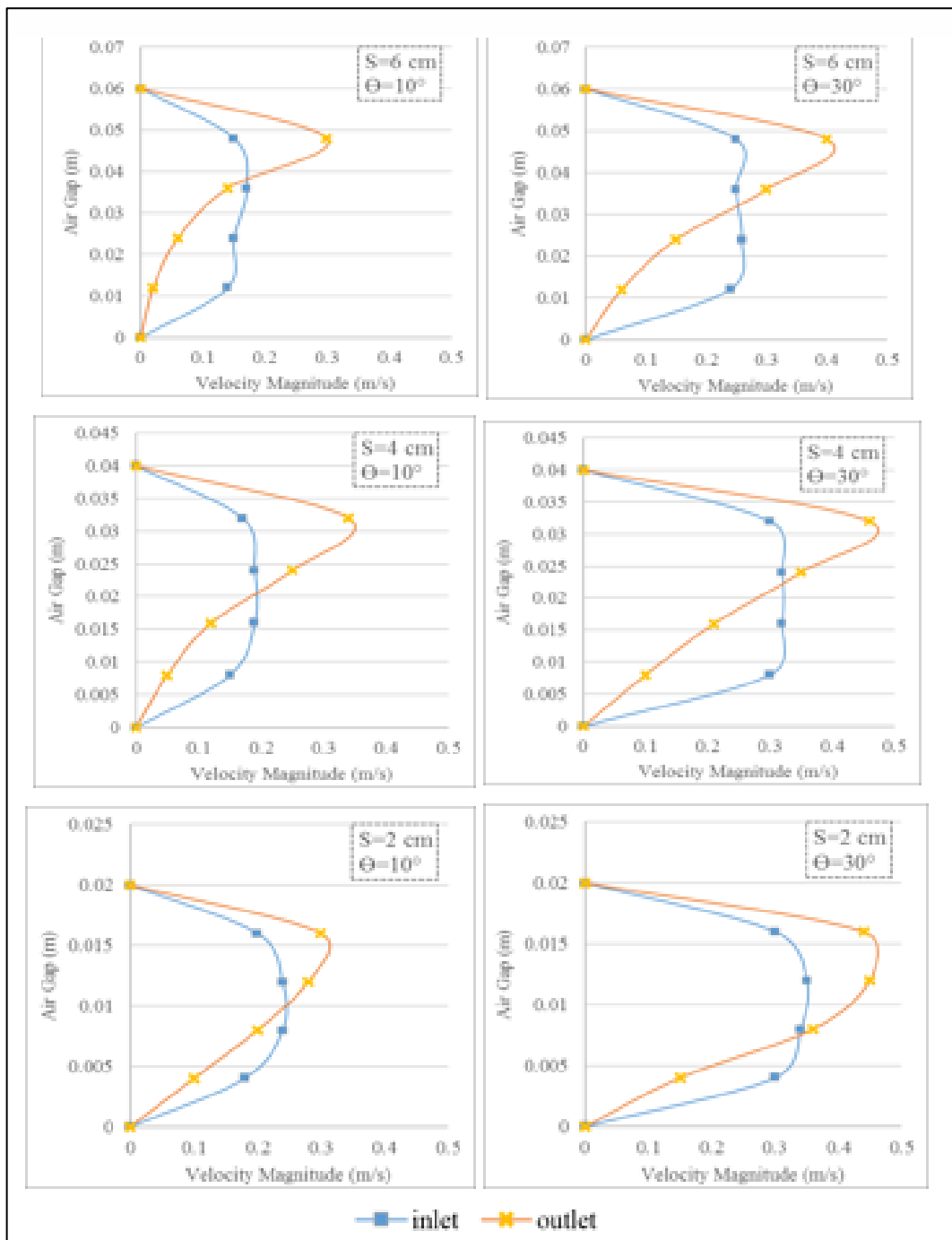


Figure 7: Velocity variation at the inlet and outlet of the channel at  $1000 \text{ W/m}^2$  radiation intensity

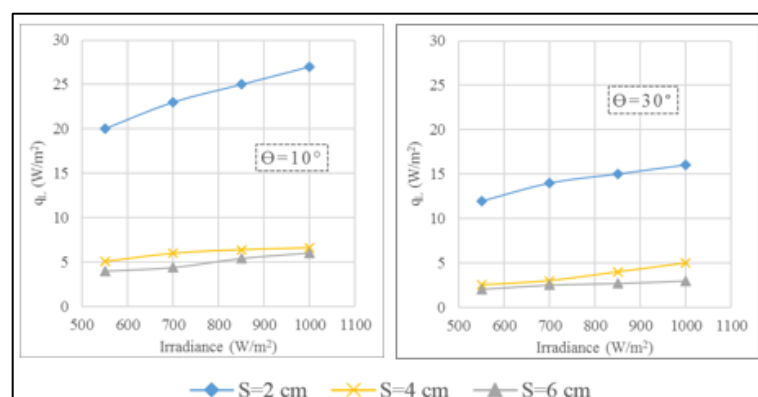


Figure 8: The transferred heat flux from the lower plate for different inclinations and air gap thicknesses

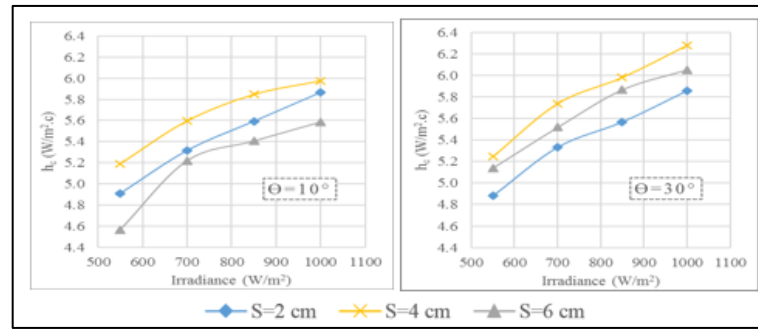


Figure 9: The convection heat transfer coefficient at the inner hot surface for different inclinations and air gap thicknesses

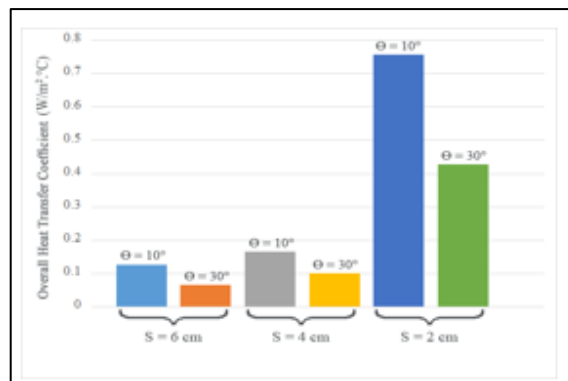


Figure 10: The overall heat transfer coefficient for different inclinations and air gap thicknesses

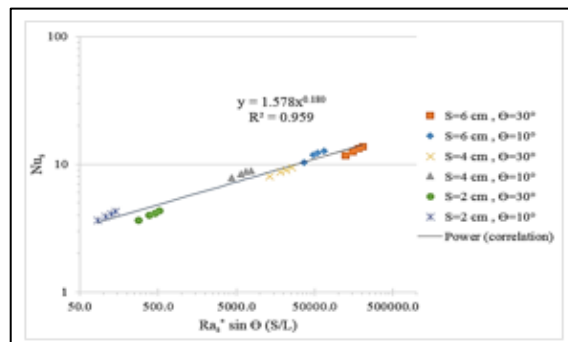


Figure 11: Correlation of  $Nu_S$  and  $Ra_S^* \sin \theta (S/L)$  for different inclinations, air gap thicknesses, and radiation intensities

VI. Experimental dimensionless correlation

The data obtained from the experiments were reduced to a single dimensionless correlation of Nusselt number ( $Nu_S$ ) as a function of the modified Rayleigh number ( $Ra_S$ ), inclination angle ( $\theta$ ), and aspect ratio defined as air gap thickness to channel length ( $S/L$ ). The method of least square was applied to the data and the correlation fitted to 96% of the data. The following correlation can be handily utilized for designing of engineering applications dealing with high temperature difference natural convection heat transfer.

$$Nu_S = 1.578 [Ra_S^* \sin \theta (S/L)]^{0.18} \tag{5}$$

4. Conclusion

An experimental investigation was performed to study the effect of inclination angle and air gap thickness on the thermal behaviour of a double skin ventilated roof model at different radiation intensities. It can be concluded that placing another roof skin with a ventilated air gap significantly reduces the roof solar heat gain. The results indicated that the higher the inclination of the roof from the horizontal, the higher the ventilation rate and hence lower heat gain through the bottom plate. As for the air gap thickness, the lower



plate should be sufficiently far from the high-temperature currents to avoid the transfer of heat from the air in the channel to the lower plate. In this study, increasing the air gap from 2 cm to 4 cm reduced the heat gain significantly but when the gap was further increased to 6 cm, the reduction in the heat flux was insignificant. An important correlation was also reduced between Nusselt number ( $Nu_S$ ) and the single parameter  $Ra_S^* \sin \theta (S/L)$ . This correlation can be handily utilized for designing of engineering applications dealing with high temperature difference natural convection heat transfer.

#### Appendix-A

##### A.1 Numerical Integration

The appropriate integration method for estimating the average temperature of the upper and lower plates is Simpson's 3/8 rule as follows [15]:

$$T_1 = \frac{T_{1.1} + 3T_{1.2} + 3T_{1.3} + T_{1.4}}{8} \quad (A.1)$$

$$T_2 = \frac{T_{5.1} + 3T_{5.2} + 3T_{5.3} + T_{5.4}}{8} \quad (A.2)$$

As for the bulk temperature of air, it is estimated by first integrating the vertical five points of each section using Boole's rule, then integrating the resulting points by Simpson's 3/8 rule as follows [15]:

$$T_{b1} = \frac{7T_{1.1} + 32T_{2.1} + 12T_{3.1} + 32T_{4.1} + 7T_{5.1}}{90} \quad (A.3)$$

$$T_{b2} = \frac{7T_{1.2} + 32T_{2.2} + 12T_{3.2} + 32T_{4.2} + 7T_{5.2}}{90} \quad (A.4)$$

$$T_{b3} = \frac{7T_{1.3} + 32T_{2.3} + 12T_{3.3} + 32T_{4.3} + 7T_{5.3}}{90} \quad (A.5)$$

$$T_{b4} = \frac{7T_{1.4} + 32T_{2.4} + 12T_{3.4} + 32T_{4.4} + 7T_{5.4}}{90} \quad (A.6)$$

$$T_b = \frac{T_{b1} + 3T_{b2} + 3T_{b3} + T_{b4}}{8} \quad (A.7)$$

#### Nomenclature

##### English Symbols

- $g$ : The gravitational acceleration ( $m/s^2$ )  
 $h_c$ : Convective heat transfer coefficient ( $W/m^2 \cdot ^\circ C$ )  
 $I$ : Radiation intensity ( $W/m^2$ )  
 $k$ : Thermal conductivity ( $W/m \cdot ^\circ C$ )  
 $L$ : The channel length ( $m$ )  
 $Nu_S$ : Nusselt number based on the spacing between the two plates  
 $q_L$ : The heat flux from the lower plate ( $W/m^2$ )  
 $q_c$ : The heat flux transferred by convection ( $W/m^2$ )  
 $q_r$ : The heat flux transferred by radiation ( $W/m^2$ )  
 $q_u$ : The heat flux from the upper plate ( $W/m^2$ )  
 $Ra_S^*$ : The modified Rayleigh number based on the spacing between the two plates  
 $S$ : The spacing between the upper and lower plates ( $m$ )  
 $T_1$ : The temperature of the upper plate ( $^\circ C$ )  
 $T_2$ : The temperature of the lower plate ( $^\circ C$ )  
 $T_b$ : The bulk temperature of air ( $^\circ C$ )  
 $T_o$ : The external temperature of air ( $^\circ C$ )  
 $U$ : The overall heat transfer coefficient ( $W/m^2 \cdot ^\circ C$ )  
 $V$ : Velocity magnitude ( $m/s$ )

##### Greek Symbols

- $\sigma$ : Stefan–Boltzmann constant ( $W/m^2 K^4$ )  
 $\varepsilon_1$ : The inner surface emissivity of the upper plate  
 $\varepsilon_2$ : The inner surface emissivity of the lower plate  
 $\theta$ : The inclination angle of the roof model from the horizontal (degree)  
 $\beta$ : Coefficient of thermal expansion ( $1/K$ )  
 $\mu$ : Dynamic viscosity ( $Pa \cdot s$ )  
 $\nu$ : Kinematic viscosity ( $m^2/s$ )  
 $\alpha$ : Thermal diffusivity ( $m^2/s$ )

#### References

- [1] J. Hirunlabh, S. Wachirapuwadon, N. Pratinthong, and J. Khedari, "New configurations of a roof solar collector maximizing natural ventilation," *Build. Environ.* Vol. 36, No. 3, pp. 383–391, 2001.  
 [2] J. Khedari, P. Yimsamerjit, and J. Hirunlabh, "Experimental investigation of free convection in roof solar collector," *Build. Environ.* Vol. 37, No. 5, pp. 455–459, 2002.

- [3] T. Bunnag, J. Khedari, J. Hirunlabh, and B. Zeghamati, "Experimental Investigation of free convection in an open-ended inclined rectangular channel heated from the top," *Int. J. Ambient Energy*, Vol. 25, No. 3, pp. 151–162, 2004.
- [4] W. Puangsombut, J. Hirunlabh, J. Khedari, B. Zeghamati, and M. M. Win, "Enhancement of natural ventilation rate and attic heat gain reduction of roof solar collector using radiant barrier," *Build. Environ.* Vol. 42, No. 6, pp. 2218–2226, Jun. 2007.
- [5] C. ming Lai, J. Y. Huang, and J. S. Chiou, "Optimal spacing for double-skin roofs," *Build. Environ.* Vol. 43, No. 10, pp. 1749–1754, 2008.
- [6] L. Susanti, H. Homma, H. Matsumoto, Y. Suzuki, and M. Shimizu, "A laboratory experiment on natural ventilation through a roof cavity for reduction of solar heat gain," *Energy Build.*, Vol. 40, No. 12, pp. 2196–2206, 2008.
- [7] Y. K. Salman and H. S. Hamad, "Laminar Natural convection heat transfer between ducted parallel plates," *J. Eng.*, Vol. 14, No. 3, pp. 2786–2803, 2008.
- [8] S. Lee, S. H. Park, M. S. Yeo, and K. W. Kim, "An experimental study on airflow in the cavity of a ventilated roof," *Build. Environ.* Vol. 44, No. 7, pp. 1431–1439, 2009.
- [9] S. Tong and H. Li, "An efficient model development and experimental study for the heat transfer in naturally ventilated inclined roofs," *Build. Environ.* Vol. 81, pp. 296–308, 2014.
- [10] B. Bokor, H. Akhan, D. Eryener, and L. Kajtár, "Theoretical and experimental analysis on the passive cooling effect of transpired solar collectors," *Energy Build.*, Vol. 156, pp. 109–120, 2017.
- [11] A. Namin, C. Jivacate, D. Chenvidhya, K. Kirtikara, and J. Thongpron, "Construction of tungsten halogen, pulsed LED, and combined tungsten halogen-LED solar simulators for solar cell I - V characterization and electrical parameters determination," *Int. J. Photoenergy*, Vol. 2012, pp. 1–9, 2012.
- [12] P. C. Chang, C. M. Chiang, and C. M. Lai, "Development and Preliminary evaluation of double roof prototypes incorporating RBS (radiant barrier system)," *Energy Build.*, Vol. 40, No. 2, pp. 140–147, 2008.
- [13] M. C. Yew, N. H. Ramli Sulong, W. T. Chong, S. C. Poh, B. C. Ang, and K. H. Tan, "Integration of Thermal insulation coating and moving-air-cavity in a cool roof system for attic temperature reduction," *Energy Convers. Manag.*, Vol. 75, pp. 241–248, 2013.
- [14] F. P. Incropera, D. P. DeWitt, T. L. Bergman, and A. S. Lavine, "Fundamentals of heat and mass transfer," Wiley, 2007.
- [15] S. C. Chapra and R. P. Canale, "Numerical methods for engineers," Seventh, Vol. 33, No. 3. McGraw-Hill Science/Engineering/ Math, 2015.